

Experimental research on overlying strata movement and fracture evolution in pillarless stress-relief mining

Junhua Xue¹ · Hanpeng Wang² · Wei Zhou¹ · Bo Ren¹ · Changrui Duan¹ · Dongsheng Deng¹

Received: 20 February 2015 / Revised: 11 March 2015 / Accepted: 15 March 2015 / Published online: 21 May 2015
© The Author(s) 2015. This article is published with open access at Springerlink.com

Abstract In multiple seams mining, the seam with relatively low gas content (protective seam) is often extracted prior to mining its overlying and/or underlying seams of high gas content and low permeability to minimize the risk of high gas emission and outbursts of coal and gas. A key to success with this mining sequence is to gain a detailed understanding of the movement and fracture evolution of the overlying and underlying strata after the protective seam is extracted. In Zhuji mine, the No. 11-2 seam is extracted as a protective seam with the pillarless mining method by retaining goaf-side roadways prior to its overlying No. 13-1 seam. An investigation has been undertaken in the panel 1111(1) of Zhuji mine to physically simulate the movement and fracture evolution of the overlying strata after the No. 11-2 seam is extracted. In the physical simulation, the displacement, strain, and deformation and failure process of the model for simulation were acquired with various means such as grating displacement meter, strain gauges, and digital photography. The simulation result shows that: (1) Initial caving interval of the immediate roof was 21.6 m, the first weighting interval was 23.5–37.3 m with the average interval of 33.5 m, and the periodic weighting interval of the main roof was in a range of 8.2–20.55 m and averaged at 15.2 m. (2) The maximum height of the caving zone after the extraction of No. 11-2 seam was 8.0 m, which was 4 times of the seam mining height and the internal strata of the caving zone collapsed irregularly. The mining-induced fractures developed 8–30 m above the mined No. 11-2 seam, which was 7.525 times of the seam mining height, the fracture zone was about 65° upward from the seam open-off cut toward the goaf, the height of longitudinal joint growth was 4–20 times of the mining seam height, and the height of lateral joint growth was 20–25 times of the mining seam height. (3) The “arch-in-arch” mechanical structure of the internal goaf was bounded by an expansion angle of broken strata in the lateral direction of the retained goaf-side roadway. The spatial and temporal evolution regularities of overburden’s displacement field and stress field, dynamic development process and distribution of fracture field were analyzed. Based on the simulation results, it is recommended that several goaf drainage methods, i.e. gas drainage with buried pipes in goaf, surface goaf gas drainage, and cross-measure boreholes, should be implemented to ensure the safe mining of the panel 1111(1).

Keywords Low-permeability coal seam · Pillarless stress-relief mining · Overburden movement · Fracture evolution · Physical simulation

1 Introduction

The permeability of coal reservoir in China is generally low. The coal seams in Huainan are typical “three-high, one-low and one soft” seams, namely high gas content in coal (12–26 m³/t), high gas pressure (up to 6.2 MPa), high rock stress (the maximum principal stress is up to 26.8 MPa), low seam permeability (0.001 mD), and soft

✉ Junhua Xue
xuejunhua2003@163.com

¹ State Key Laboratory of Deep Coal Mining & Environment Protection, Huainan 232001, China

² Geotechnical & Structural Engineering Research Center, Shandong University, Jinan 250012, China

coal strength (Yuan 2006). The complex geological conditions pose serious threats to coal mining. In high gas seams, gas must be extracted before coal mining, however the low permeability of coal seams seriously affects the gas drainage effect. Based on the geological conditions of the coal seams in Huainan mining area, the technology of integrated coal production and gas extraction was innovated by Yuan Liang through mining a protective seam with retained goaf-side roadways and “Y” type ventilation system. A key of the technology is to significantly increase the permeability of the overlying and underlying protected seams and subsequent gas extraction from the protected coal seams by boreholes drilled from the retained roadways (Yuan 2008). The technology of integrated coal production and gas extraction requires a detailed understanding of the deformation and failure of the surrounding rocks in working faces and gas migration and enrichment in and around the working faces, especially the fracture evolution of overlying strata after the protective seam is extracted as the fracture distribution significantly affects the target zones of gas drainage by boreholes.

A large number of studies have been undertaken to understand in the mining-induced fracture distribution in overlying strata (Karmis et al. 1983; Hasenfus et al. 1988; Bai and Elsworth 1990; Shu and Bhattacharyya 1993; Palchik 2002; Unver and Yasitli 2005; Cao et al. 2011; Li et al. 2012; Usanov et al. 2013; Liu et al. 2014). It is generally recognized that overlying strata in longwall extraction can be divided into three different zones: caving zone, fracture zone and continuous deformation zone. Qian et al. (2003) established the key strata theory in ground control. Song (1988) proposed the theory of transferring rock beam. Liu (1995) attributed the damage of overlying rock strata to “three zones”, respectively caving zone, fracture zone and continuous deformation zone, and put forward the general understanding of “three horizontal zones” and “three vertical zones”. Based on the findings of the simulation test, Deng et al. (1998), Guo et al. (2009) and Guo et al. (2012) obtained the evolution characteristics of mining fracture regularity and fractured rock mass. Xue and Xue (2012), Li et al. (2012) and Li and Zhang (2011) developed a method to predict the propagation height of mining induced fractures, the height of fractured zone in top coal caving mining, and the non-steady state evolution of fractures. They also revealed the development of two types of fractures in overlying strata: delamination fractures and vertical fractures. Most of the above-mentioned studies were undertaken in normal mining depth, as mining depth increases ground stress becomes quite high and the pore forming rate and effective drainage time are relatively low (Palchik 2005; Li 2012; Szlazak et al. 2014). Physical modeling test has been undertaken to simulate the goaf-side roadway retaining process in mining the first panel

1111(1) of the protective No. 11-2 seam at Zhuji mine in Huainan mining area. This paper presents the test findings, including the spatial and temporal evolution regularities of overburden’s displacement and stress fields, and dynamic development process and distribution of overburden’s fracture field.

The annual production Zhuji mine is 4.0 million tons and current mining seams are No. 11-2 seam and No. 13-seam. The No. 11-2 seam lies about 65 m below the No. 13-1 seam. Both seams are outburst prone. The 11-2 seam is mined as a protective seam to protect the No. 13-1 seam (protected seam). The No. 11-2 seam is 1.26 m thick on average, flat, and contains an average gas content of 4.95 m³/t. The No. 13-1 seam lies 65 m above the No. 11-2 seam and has an average gas content of 6.98 m³/t. The first extraction panel 1111(1) is in the No. 11-2 seam and has a mining depth of about 910 m. The panel is 220 m wide and 1618 m long. The panel is mined with the fully-mechanized longwall retreat method. A goaf-side roadway is retained (pillarless mining) and Y type ventilation is adopted for the panel extraction (Lu et al. 2013) (Fig. 1).

A physical model was made to simulate the panel 1111(1), as shown in Fig. 2. The simulation test was performed with high-stress modeling system. The system has double gantry structure and double cylinder installation. The test conditions of plane strain and plane stress were simulated by installing or removing the front and rear rigid reaction beam devices.

The touch-screen hydraulic loading control system was used to achieve synchronous non-uniform gradient loading and long loading. The model strain and displacement were obtained with a number of high-tech equipment such as high speed static strain test system, micro-precision grating displacement meter, digital cameras measuring systems, and high-precision total station test.



Fig. 1 Zhuji mine in China



Fig. 2 High stress model test system

The model block size was 2000 (W) × 2000 (H) × 650 (T) (mm × mm × mm) and the ground stress field was achieved by external compensation method, the maximum output horizontal and vertical direction of cylinders were 3000 kN, and the maximum load intensity was 2.23 MPa.

2 Test

2.1 Test purpose

The retained goaf-side roadway is subject to repeated collapse of its lateral rock strata and continuous disturbance, the movement and crack development characteristics of goaf overburden are very important to the roadway stability and dictate the gas rich region and drainage position.

A plane stress model was used in the test to simulate excavation directions in both the strike direction and the dip direction, thus overlying strata movement characteristics can be more thoroughly studied.

2.2 Test model

The simulated model dimension was 2.0 m × 2.0 m × 0.65 m (width × height × thickness). The model simulates the strata size of 120 m × 120 m (width × height) with the geometric similarity ratio of 60:1.

The pillarless mining physical simulation model is shown in Fig. 3. A total of 23 rock strata were laid in the model, containing three coal seams: No. 11-2 seam, No. 11-1 seam, and No. 13-1 seam. The No. 11-2 coal seam was 61.8 m below the No. 13-1 seam and 4.5 m above the No. 11-1 seam. A pillar of 200 mm wide was retained on mining boundaries of modeled working face and a pillar of 583 mm wide was retained on coal side to ensure similarity of the boundary conditions. In the model, a mining height was 35 mm, excavation length was 1100 mm; the cross-sectional dimension of the goaf-side retained roadway was

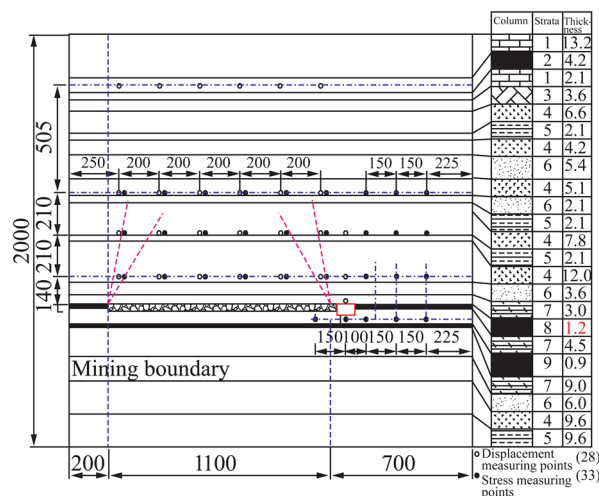


Fig. 3 Test model layout and strata histogram

83.3 mm × 50 mm (width × height), the left lane dimension of the roadway was 66.7 mm × 50 mm (width × height) and the support side lane of the roadway was 50 mm in width.

The average density of the actual rock was 2.5 g/cm³, the average density of the simulated rock was 1.5 g/m³, and density similarity ratio was 5:3. Stress similarity constant was then calculated as 100 while similarity constants of rock tensile strength σ_c , compressive strength σ_f , bending strength σ_b , shear strength σ_s and elastic modulus E were all at 100.

As the modeled mining depth was 910 m, the vertical stress of roadway original rock $\sigma_{vp} = 22.75$ MPa, and horizontal stress $\sigma_{Hp} = 11.4$ MPa, therefore the vertical and horizontal stress in the model were set at $\sigma_{vm} = 0.23$ MPa, $\sigma_{Hm} = 0.11$ MPa respectively.

The strata numbered from 1 to 9 in Fig. 3 represents mudstone, No. 13-1 coal seam, sandy shale, No. 1 mudstone, siltstone and fine sandstone, No. 2 mudstone, No. 11-2 coal seam, No. 11-1 coal seam, and other rock strata, respectively.

2.3 Simulation materials

The fundamental forces that the overlying strata bear are the tension and compression, their damage take the form of shear and tensile failure, the deformation and failure of the strata are related to their elastic modulus, Poisson's ratio and strength. Therefore simulation materials were selected by similarity conditions as follows: sand of particle size less than 1.5 mm as aggregate, gypsum and lime bound with water, mica powder as a laminated material to simulate rock strata structure. Specific rock strata parameters are in Table 1.

Table 1 Physical and mechanical parameters of rocks

Strata No.	Lithology	Height (mm)	Density (kg/m ³)	Compressive strength σ_{cm} (Mpa)
1	Mudstone	220	1650	0.18
2	No. 13-1 coal seam	70	1650	0.08
3	Sandy mudstone	60	1650	0.25
4	Mudstone	110	1650	0.20
5	Siltstone	35	1650	0.32
6	Fine sandstone	90	1650	0.45
7	Mudstone	50	1500	0.18
8	No. 11-2 coal seam	20	1500	0.08
9	No. 11-1 coal seam	15	1500	0.08

2.4 Testing procedures

The simulation test was carried out with the following procedures:

- (1) Making the modeled rock layer by layer, tamping and burying displacement and strain sensors in pre-determined position until the model was completed.
- (2) Removing the front and rear modules after the completed model was ready for 15 days, marking the grid of 100 mm × 100 mm, and then let the model dry naturally for 7 more days.
- (3) Connecting the sensor lines to their respective instrument, testing the data acquisition system to make sure that it operate normally.
- (4) Applying boundary stress through the hydraulic system to compensate simulated stress field and allow it stabilizing for 3 days.
- (5) Excavating the roadway, recording surrounding rock deformation.
- (6) Opening a gap beside the roadway, filling the gap, and letting it dry naturally for 1 day.
- (7) Excavating along the edge of the filled gap along the direction of mining boundary, excavating 9 cm (equivalent to 5.4 m in actual roadway development rate), continue to excavate every 5 min, recording the time of each excavation, observing and photographing after each excavation, while recording deformation and stress data until excavation reached the mining boundary line.

3 Analysis of test results

3.1 Goaf overburden fracture growth evolution

In the test, the whole process was photographed with a high resolution digital single-lens reflex (SLR) camera (Fig. 4)

and the overburden movement and fracture evolution of the pillarless mining can be clearly seen.

As you can be seen in Fig. 4 that when the longwall face in the model retreated 36 cm or 21.6 m in the field, the immediate roof mudstone was caved in; when the retreating distance in the model was 54 cm or 32.4 m in the field, the immediate roof mudstone was caved in for the second time; when the distance in the model was 63 cm or 37.8 m in field, the fine sandstone layer of the basic roof initially was caved in and the first weighting occurred; when the distance in the model was 72 cm or 43.2 m in field, the siltstone layer of the main roof was caved in, bed-separated fractures of the overlying stratum began to develop; when the distance in the model was 99 cm or 59.4 m in the field, the fine sandstone layer of the basic roof was caved in second time, the initial periodic weighting interval of the main roof was measured to be 15.6 m in the field, a wide range of lateral and longitudinal fractures were developed above the main roof, the maximum height of bed separation fractures above the coal seam was 35 cm; the fine sandstone layer of basic roof was caved for the third time after the face stopped for 1 day, the second periodic weighting interval of the main roof was 14.8 m in the field, the height of bed separation fractures above coal the seam was 50 cm, some lower fractures were closed, bending zone, fracture zone and caving zone were clearly observed.

The maximum height of the caving zone was 9.0 m, which was 7.5 times of the mining height. The rock blocks in the caving zone were irregularly shaped. The height of mining-induced fractures was from 8.0 to 30 m, 7.5–25 times of the mining height. The bed separation fractures in the lower fracture zone were obvious. The fracture zone was about 65° upward from the face to goaf direction. The height of the longitudinal fractures was 4–20 times of the mining height. The height of the lateral fractures was 20–25 times of the mining height. The bending zone was above the fracture zone. The height of the bending zone

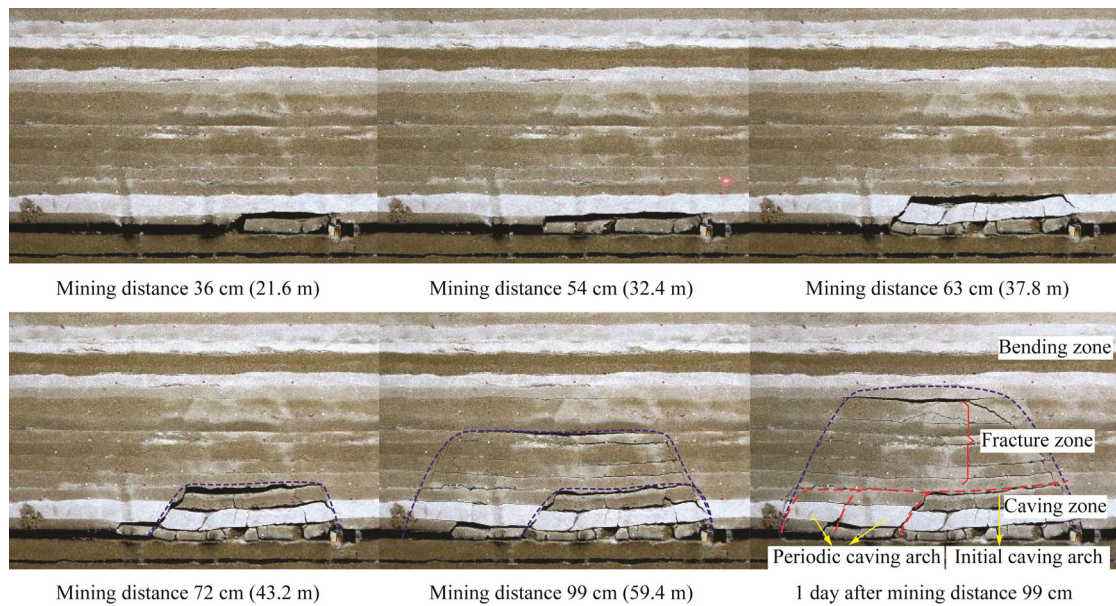


Fig. 4 Overburden movement and fracture evolution in pillarless mining

was more than 25 times of the mining height. The rock strata movement in bending zone was observed to be continuous. Generally, the stress-relieved coal seam was usually dominated by transverse fractures and swelled longitudinally. There was no longitudinal fracture between bending zone and fracture zone.

These results suggest that, the roof on the goaf side of the retained roadway broke in the form of “cantilever” because of the support of filling wall. The unanchored end of the cantilever was in upper direction and on the outer side of filling wall. There wasn’t significant deformation and failure in the roof of the retained roadway, indicating that the filling wall could ensure the stability of a retained roadway. In inclination direction, the “arch-in-arch” structure space-time evolution existed in the pillarless mining. The initial caving arch and periodic caving arch constituted the lower arch, the overlying fracture zone and bending zone made up the upper arch, the lower arch was contained within the upper arch, and the upper arch expanded constantly in the longitudinal and vertical directions in which the lower arch moved forward at the same time.

3.2 Displacements

Rock strata displacements obtained by the multi-point displacement meter and total station were shown in Figs. 5 and 6.

As can be seen from Fig. 5 that the roof displacement at the level of 52 cm above the coal seam was very small, suggesting the height of caving zone of 50 cm. Roof displacement at the level of 12 cm above the coal seam with

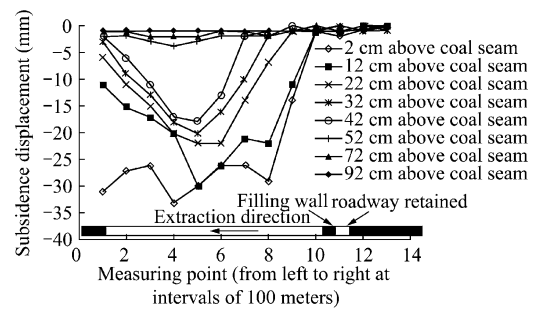


Fig. 5 Roof displacement distribution at different heights

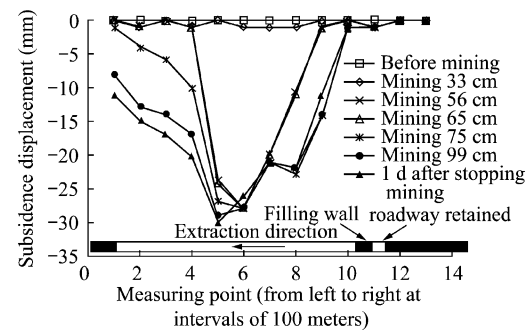


Fig. 6 Displacement at the level of 12 cm above the seam with excavation step

excavation step is shown in Fig. 6. As can be seen from Fig. 6 that the area 0–15 m ahead the working face was intensively affected by mining, the velocity of convergence increased fast between the two sides of roof and floor; the area of 15–45 m ahead the working face was also affected

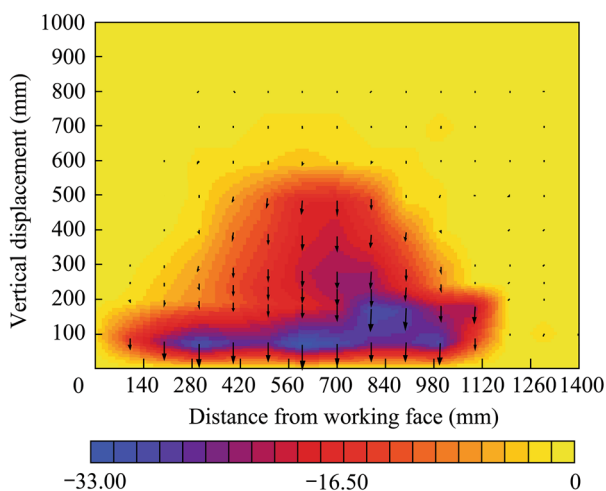


Fig. 7 Roof vertical displacement contour and vector

by mining to some extent but much less than the area 0–15 m ahead of the face, and the area 70 m ahead the face was basically unaffected by mining.

Figure 7 shows the roof vertical displacement contour and vector. The color in the figure represents the intensity of displacement and fractures, and the dart colour means relatively more displacement and fractures.

3.3 Analysis of strain field

Figure 8 shows the strain field distribution, vertical strain and shear strain contour. As can be seen from the vertical strain contour that the tensile strain was larger as strata breakage and fracturing was developing in caving zone and fracture zone. As can be seen from shear strain contour that there was obvious shear strain zonal distribution upward at the working face inclined toward mining direction and above goaf on the side of the retained roadway.

3.4 Roof movement characteristics on goaf side

According to the results of the simulation test, overburden fracture region can be divided into three zones: fracture initiation and development zone, fracture closure zone, and fracture stable development zone. The specific overlying strata structure movement characteristics related to these fracture zones are shown in Fig. 9.

As can be seen in Fig. 9 that there were rupture-dilative rock areas along the goaf-side direction of the retained roadway which was bounded by rupture line, that was the fracture stable development zone defined in previous section. The overlying strata caving form in goaf under the retained roadway was similar to that of open-off cut on the goaf side. The roof periodic caving phenomenon did exist in both directions of the working face. Roof on the goaf

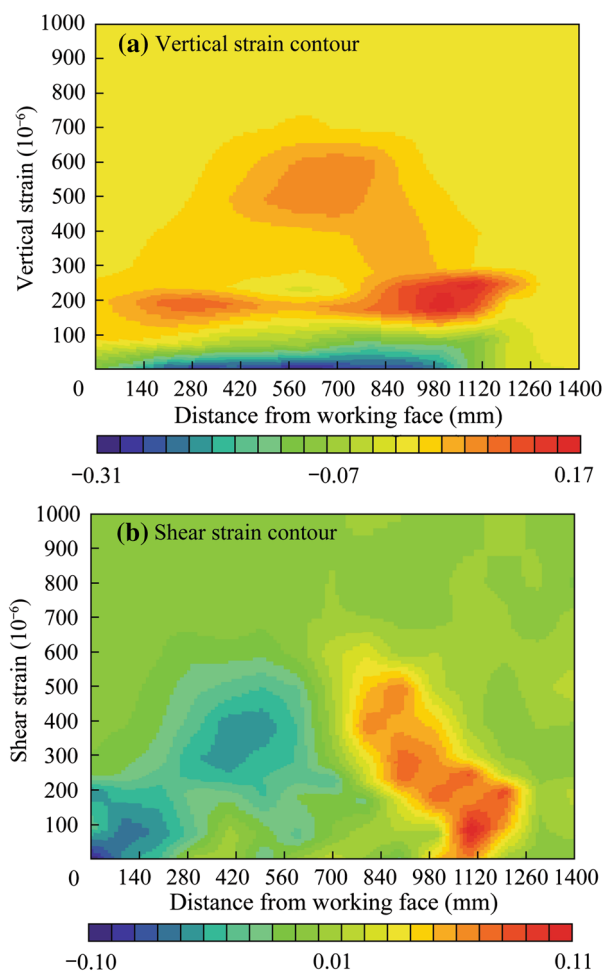


Fig. 8 Roof vertical strain and shear strain contour

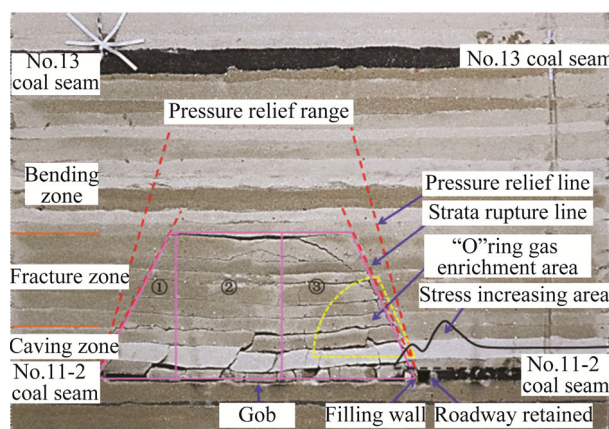


Fig. 9 Overburden movement characteristics of pillarless mining

side under the retained roadway broke in the form of “cantilever” and layered caving. The cantilever breaking point acted as a rotation axis of the overlying strata. Due to differences in the physical, mechanical and geometric

parameters, the breaking period of the overlying strata varies, resulting in the formation of a stable structure of fracture development, and this structure can't be compacted because of lateral stability region balanced action. The fracture closure zone exists in the middle of goaf. The fracture stable development zone is on the side of retained roadway. A fan-shaped fracture region is formed in this area (or "O" ring), which is also gas accumulation area.

Fracture initiation and development zone is close to the rear side of working face, and the difference with the fracture stable development zone is that the former is still in initiation and development process because of the continuous stopping. The fracture closure zone is between the fracture initiation and development zone and the fracture stable development zone. The fracture closure zone evolves from the fracture initiation and development zone.

Stress relief in protected No. 13 seam occurred between stress relief lines due to lower strata subsidence, thus "stress relief and permeability enhancement" effect appeared in stress relief zone, resulted in significant increase in the permeability of rock and coal seam in this zone. Effective gas drainage of high flow and purity should be obtained in the "O" ring and stress relief zone.

3.5 Engineering application of test results

Gas drainage has proven to be an effective method to control gas emission and outbursts of coal and gas in underground coal mining (Black and Aziz 2009; Yuan 2010; Karacan et al. 2011). Based on the simulation test, gas control measures were developed to manage gas issues in panel 1111(1). These measures included mainly goaf gas drainage with buried pipes in the goaf, surface vertical wells, and cross-measure boreholes. The return air volume was 2290–2700 m³/min during gas drainage period. Gas concentration in return air was less than 0.6 %. Gas extraction rate in the working face was more than 60 %. The average gas extraction rate was 70 %. With these gas control measures, panel 1111(1) was mined without encountering any gas-related safety issues. With stress relief mining of No. 11-2 coal seam, the protected area of No. 13 coal seam was extensively de-stressed and de-gassed. The risk of coal and gas outburst during both development of headings and panel extraction was minimized, and a significant gain was achieved in the production of panel 1111(1).

4 Conclusions

An investigation was undertaken in the panel 1111(1) of Zhuji mine to physically simulate the movement and fracture evolution of the overlying strata after the No. 11-2 seam was extracted. In the physical simulation, the displacement, strain, and deformation and failure process of

the model for simulation were acquired with various means such as grating displacement meter, strain gauges, and digital photography. The simulation results showed that:

1. Initial caving interval of the immediate roof was 21.6 m and the first weighting interval was from 23.5 to 37.3 m (33.5 m on average). Periodic weighting interval of the main roof varied between 8.2 and 20.55 m (15.2 m on average).
2. The maximum height of the caving zone after No. 11-2 seam was mined was 8.0 m or 4 times of mining height, and internal strata of the caving zone collapsed irregularly. The mining-induced fractures developed 8.0–30 m above the mined No. 11-2 seam, which was 7.525 times of the seam mining height, the fracture zone was about 65° upward from the seam open-off cut toward the goaf, the height of longitudinal joint growth was 4–20 times of the seam mining height, the height of lateral joint growth is 20–25 times of the seam mining height.
3. The spatial and temporal evolution regularities of overburden's displacement field and stress field, dynamic development process and distribution of fracture field were analyzed and it was found that there was an "arch-in-arch" mechanical structure of internal goaf bounded by expansion angle in the lateral direction of the retained goaf-side roadway.
4. Based on the simulation results, it is recommended that several goaf drainage methods, i.e. gas drainage with buried pipes in goaf, surface goaf gas drainage, and cross-measure boreholes, should be implemented to ensure the safe mining of the panel 1111(1).

Acknowledgments The program was supported by the National Natural Science Foundation of China (51427804) and the Open Found of State Key Laboratory of Deep Coal Mining & Environment Protection.

Open Access This article is distributed under the terms of the Creative Commons Attribution 4.0 International License (<http://creativecommons.org/licenses/by/4.0/>), which permits unrestricted use, distribution, and reproduction in any medium, provided you give appropriate credit to the original author(s) and the source, provide a link to the Creative Commons license, and indicate if changes were made.

References

- Bai M, Elsworth D (1990) Some aspects of mining under aquifers in China. *Min Sci Technol* 10(1):81–91
- Black DJ, Aziz NI (2009) Developments in coal mine methane drainage and utilisation in Australia. In: *Proceedings of the Ninth International Mine Ventilation Congress*. Department of Mining Engineering, Indian School of Mines University, Dhanbad, India, 10–13 Nov 2009, pp 445–460

- Cao AY, Dou LM, Li FC, Jiang H, Qu Y, Han RJ (2011) Study on characteristic of overburden movement in unsymmetrical isolated longwall mining using microseismic technique. *Procedia Eng* 26:1253–1262
- Deng KZ, Zhou M, Tan ZX, Xu NZ (1998) Study on laws of rock mass breaking induced by mining. *J China Univ Min Technol* 27(3):261–264
- Guo GL, Zha JF, Miao XX, Wang Q, Zhang XN (2009) Similar material and numerical simulation of strata movement laws with long wall fully mechanized gangue backfilling. *Procedia Earth Planet Sci* 1(1):1089–1094
- Guo H, Yuan L, Shen BT, Qu QD, Xue JH (2012) Mining-induced strata stress changes, fractures and gas flow dynamics in multi-seam longwall mining. *Int J Rock Mech Min Sci* 54:129–139
- Hasenfus GJ, Johnson KL, Su DWH (1988) A hydro geomechanical study of overburden aquifer response to long wall mining. In: *Proceedings of the 7th conference of ground control in mining*, pp 144–152
- Karacan CÖ, Ruiz AF, Cotè M, Phipps S (2011) Coal mine methane: a review of capture and utilization practices with benefits to mining safety and to greenhouse gas reduction. *Int J Coal Geol* 86(2-3):121–156
- Karmis M, Triplett T, Haycocks C, Goodman G (1983) Mining subsidence and its prediction in Appalachian coalfield. *Rock Mech* 22:665–675
- Li YB (2012) Study on the integrated pillarless coal production and methane extraction technology. *Adv Mater Res* 1792(524):735–738
- Li K, Zhang YB (2011) Research on overlying strata movement and deformation under the conditions of shortwall and longwall mining. *Appl Mech Mater* 1446(90):1299–1302
- Li CY, Chen J, Wu HF (2012) Field measurement research on overburden stratum movement and deformation. *Appl Mech Mater* 170:1151–1157
- Liu TQ (1995) Influence of mining activities on mine rockmass and control engineering. *J China Coal Soc* 20(1):1–5
- Liu JK, Dong C, Zhang SQ, Zhang Y (2014) Research on the rules of overlying rock movement by similar material simulation in fully mechanized top coal caving mining with high cutting height. *Appl Mech Mater* 3013(522):1419–1425
- Lu P, Fang LC, Tong YF, Li GH, Zhang GF, Deng Z (2013) Relieved gas drainage and comprehensive control in gob of Y-type coal face in the first coal seam mining of deep multi-seams. *J Min Saf Eng* 30(3):456–462
- Palchik V (2002) Influence of physical characteristics of weak rockmass on height of caved zone over abandoned sub-surface coalmines. *Environ Geol* 42(1):92–101
- Palchik V (2005) Localization of mining-induced horizontal fractures along rock layer interfaces in overburden: field measurements and prediction. *Environ Geol* 48:68–80
- Qian MG, Miao XX, Xu JL (2003) Dominant stratum theory for control of strata movement. China University of Mining and Technology Press, Xuzhou
- Shu DM, Bhattacharyya AK (1993) Prediction of sub-surface subsidence movements due to underground coal mining. *Geotech Geol Eng* 11(4):221–234
- Song ZQ (1988) Practical ground pressure control. China University of Mining and Technology press, Xuzhou
- Szlazak N, Obracaj D, Swolkien J (2014) Methane drainage from roof strata using an overlying drainage gallery. *Int J Coal Geol* 136:99–115
- Unver B, Yasitli NE (2005) Modelling of strata movement with a special reference to caving mechanism in thick seam coal mining. *Int J Coal Geol* 66(4):227–252
- Usanov SV, Mel'nik VV, Zamyatin AL (2013) Monitoring rock mass transformation under induced movements. *J Min Sci* 49(6):913–918
- Xue JH, Xue S (2012) Retaining a goaf-rdge gateroad in a three-entry panel layout. *Adv Mater Res* 1792(524):681–685
- Yuan L (2006) Key technique to high efficiency and safe mining in highly gassy mining area with complex geologic condition. *J China Coal Soc* 31(2):174–178
- Yuan L (2008) Key technique of safe mining in low permeability and methane-rich seam group. *Chin J Rock Mech Eng* 27(7):1370–1379
- Yuan L (2010) Concept of gas control and simultaneous extraction of coal and gas. *China Coal* 6:5–12